Accepted Manuscript

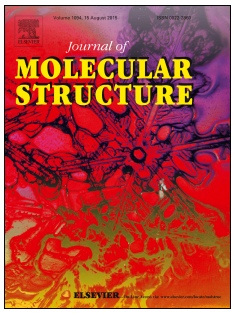

Structural, magnetic and vibrational characterization of the new organic-inorganic hybrid material, $(C_9H_{14}N)_2CoCl_4$

F. Issaoui, W. Amamou, M. Bekri, F. Zouari, E. Dhahri, M.A. Valente

PII: S0022-2860(19)30431-4

DOI: https://doi.org/10.1016/j.molstruc.2019.04.036

Reference: MOLSTR 26408

To appear in: *Journal of Molecular Structure*

Received Date: 15 February 2019

Revised Date: 14 March 2019

Accepted Date: 8 April 2019

Please cite this article as: F. Issaoui, W. Amamou, M. Bekri, F. Zouari, E. Dhahri, M.A. Valente, Structural, magnetic and vibrational characterization of the new organic-inorganic hybrid material, (C9H14N)2CoCl4, (2019), doi: 10.1016/j.molstruc.2019.04.036

Structural, magnetic and vibrational characterization of the new organic-inorganic hybrid material, $(C_9H_{14}N)_2CoCl_4$

F. Issaoui[a,c], · W. Amamou[b] M Bekri[d], F. Zouari[b], · E. Dhahri[a] and M. A. Valente[e]

[a]*Laboratoire de Physique Appliquée, Faculté des Sciences, B.P. 1171, 3000 Sfax, Université de Sfax, Tunisie*
[b]Laboratoire des Sciences des Matériaux et d'Environnement, Faculté des Sciences de Sfax, 3000 Sfax, Tunisia
[c]*Faculté des Sciences et Techniques de Sidi Bouzid, Campus Cité Agricole 9100, Université Kairouan, Tunisia*
[d]Physics Department, Rabigh College of Science and Art, King Abdulaziz University, P.O. Box 344, Rabigh 21911, Saudi Arabia
[e]Departamento de Física - Universidade de Aveiro, 3810-193 Aveiro Portugal

Abstract

A new organic–inorganic hybrid material, bis (N, N-dimethylbenzylammonium) tetrachlorocobaltate (II), $(C_9H_{14}N)_2\,CoCl_4$ was synthesized and analyzed by X-ray diffraction. Magnetization was used to investigate the magnetic properties. The structure was determined at room temperature in the triclinic space group P-1 with the following parameters: a=10.491(5)Å, b =14.207(2)Å, c =16.187(3)Å, α= 87.76(3)°, β=88.436(8)°, γ= 89.897(10)° and Z= 2. The structure can be described by the alternation of organic-inorganic layers parallel to (110) plan. The different components are connected by the N-H…Cl hydrogen bonds between the cation and the anionic group $[CoCl_4]^{2-}$. Raman and infrared spectra were used to gain more information of the title compound. An assignment of the observed vibration modes is reported. This compound exhibits an antiferromagnetic (AFM) to paramagnetic (PM) phase transition at a temperature (T_N) lower than 2 K. The values of paramagnetic Curie–Weiss temperature θ_{CW}, the nearest neighbor interaction Jnn, the classical nearest neighbor J^{cl} and the dipolar D_{nn} interactions' emphasize the existence of an antiferromagnetic interaction between the neighboring cobalt ions.

Keywords: Organic-inorganic hybrid; Magnetic properties; Chlorocobaltate (II); Thermal studies, Crystal structure.

1. Introduction

Extensive studies have been made on hybrids materials over the past decade [1-5]. In contrast,the organic-inorganic hybrid materials based on metal halide units have inspired great interests for scientific study and device application due to their optical, electronic, and magnetic properties [6-13], easy structural tunability and excellent processability. Recently, much attention was paid to the magnetic properties of hybrid compound based on transition metal (e.g. Cu, Co and Mn) halide [14-16]. In contrast, the hybrids based on cobalt halide possess good solubility and stability. The use of hydrogen bonding interactions with metal salts to control the crystal structure product has also recently received attention. Brammer and Orpen and their co-workers have utilized supramolecular synthons (such as N–H…Cl hydrogen bonds) to form organic-inorganic hybrid crystalline solids containing organic cations and anionic metal complexes [17-19]. However, the studies concerning this kind of hybrid material is still rare so far except of studies on structural phase transition and magnetic properties of these crystals [20, 21].

Considering the attractive properties and attributes of halogenocobaltates (II) and the new promising opportunities they may open with regard to the development of useful organic-inorganic hybrid materials, the present study reports on the synthesis and structural characterization of the $(C_9H_{14}N)_2CoCl_4$ compound by X-ray diffraction , differential scanning calorimetry (DSC) and thermogravimetric analysis (TGA). The spectroscopic properties and magnetic susceptibility of the compound are discussed.

2. Experimental

2.1. Synthesis

Single crystals of the title compound were obtained by slow evaporation, at room temperature as follows: $CoCl_2.6H_2O$ (0.4 g) was dissolved in an aqueous solution of HCl (37%). The N, N-dimethylbenzylamine (0.5 ml) was dissolved in a minimum of distilled water. The mixture was stirred and remained clear without any precipitation. The resulting aqueous solution was then kept at room temperature. Within few weeks, blue parallelepipedic monocrystals suitable for X-ray investigation were grown.

2.2. X-ray data collection and structure determination

The X-ray diffraction intensities from a single crystal were collected with a Bruker Apex II Kappa CCD diffractometer employing Mo-Kα radiation (λ = 0.71073 Å). Crystal data, data collection and refinement parameters are reported in Table 1.

Intensity data were corrected for absorption effects by the Multi-scan method using the SADABS [22] program. The structure was solved by direct methods and refined by the least-squares analysis using SHELX97-2 [23]. All non-H atoms were located from successive difference Fourier Maps. All the hydrogen positions of the protonated cation were placed geometrically and held in the riding mode (the C-H and N-H bonds were fixed at 0.93 and 0.86 Å, respectively).

2.3. Characterization

The IR spectrum was recorded in the 400-4000 cm^{-1} range with a "Nicolet Impact 410" spectrometer using a simple dispersed pure KBr pressed into a pellet. The Raman spectrum was measured with a LABHARAM HR 800 triple monochromatic in the 80-4000 cm^{-1} region. The spectral slit widths were set to maintain a resolution of approximately 3 cm^{-1}. The excitation light was a 632.81 nm line of He-Ne (20mV) ion laser. Measurements were carried out under a microscope in an open furnace (under air and at ambient pressure).

Thermogravimetric analysis (TGA) was performed in air atmosphere with a heating rate of 10 °C/min from 30 to 225 °C, using an ATG PYRIS 6 instrument. The differential

scanning calorimetry analysis was performed using a DSC 822 METTLER TOLEDO instrument for temperatures ranging from 30 to 250 °C at a heating rate of 10 °C min^{-1}.

2. 4. Magnetic measurements

The magnetic susceptibility for the prepared sample was measured using a Foner magnetometer equipped with a super-conducting coil under different magnetic field. Magnetic susceptibility was measured in the temperature range of 2–300 K under different magnetic fields.

3. Results and discussion

3. 1. Structure description

According to the results of single-crystal X-ray diffraction analysis, the compound $(C_9H_{14}N)_2CoCl_4$ crystallizes in the triclinic system with space group P-1. The asymmetric unit in the relevant crystal structure contains two $[CoCl_4]^{2-}$ anion and four independent units of protonated (N, N-dimethylbenzylamine) for charge compensation (*Fig. 1*).

A projection of the structure on the (010) plane (*Fig. 2*), shows that the $CoCl_4$ tetrahedron form two infinite zigzag one-dimensional chains along the b axis located in the (a, c) planes at approximately z = 0 and z = 0.5, with the M···M···M angle between three successive cobalt atoms along the chain is 116.21(2) °, between which are intercalated the organic entities $(C_9H_{14}N)^+$.

The $(CoCl_4)^{2-}$ anion adopts a slightly distorted tetrahedral geometry, with the Co (II) ion is surrounded by four chlorine atoms, with the Co−Cl bond distances ranging from 2.223(3) to 2.302(3) Å and the Cl−Co−Cl bond angles ranging from 106.63(11) to 114.84(19)°, the geometrical features of $(CoCl_4)^{2-}$ entities are reported on (table 2). These lengths fall within the range of total observation of cobalt-halide distances reported by Chang et al. [24], and they are similar to those usually found for analogous compounds containing the tetrachlorocobaltate (II) anions. Taking into account bond lengths and angles within the

organic ions and considering the calculated average values of the Baur distortion indices [25], we deduce that all $CoCl_4$ tetrahedral are slightly distorted. The interatomic distance between the two nearest cobalt atoms is 8.215(8) Å. The nearest non-bonded distances between the cobalt and halogen atom is 6.132(8) Å, too far to allow the formation of a dimeric unit with Co–Cl–Co bridges.

The organic molecule exhibited a regular spatial configuration with normal C-C and C-N distances and C-C-C and C-C-N angles. While the C-C bond lengths of the C_6-ring varied from 1,310(16) to 1,556(17) Å, the main value of the C-N length of the [$-CH_2$-NH-$(CH_3)_2$] arms was 1.494(5) Å. Those values are comparable to the corresponding values previously reported for similar complex [26]. The packing of $(C_9H_{14}N)_2CoCl_4$ viewed (*Fig. 2*) shows alternating organic and inorganic layers along the b-axis, with the organic molecule exhibiting different orientation. The organic species interact with the $(CoCl_4)^{2-}$ anion via N–H...Cl hydrogen bonds forming a three dimensional network. Details of the hydrogen bonding interactions are listed in (Table 3).

3.2. Thermal studies

In order to examine the thermal stability of the compound, the thermogravimetric (TG) and the differential scanning calorimetry (DSC) were carried out in the temperature range of 25–350 °C and the thermogram are depicted in *Fig. 3*.

The TG curve can be described as a process of two major steps between 30 ° C temperature and 225 ° C. It shows that $(C_9H_{14}N)_2CoCl_4$ is stable up to 148 ° C, the melting points is accompanied by simultaneous decomposition of this material. A single mass loss is observed between 148 and 218 ° C. It is in good agreement with the expected value for the degradation of organic molecules (57.8% observed; 58.1% calculated). The DSC thermogram of the compound $(C_9H_{14}N)_2CoCl_4$ is registered under an argon atmosphere using a mass of 9.5

mg sample heated up to 250 ° C. It shows a single endothermic peak located at 148 °C, which corresponds to the melting compound. The value of the enthalpy calculated from the peak area is $\Delta H = 43.67$ kJ mol^{-1}.

3.3. Vibrational studies

In the present investigation, Raman and Infra-red spectroscopic studies of $(C_9H_{14}N)_2CoCl_4$ have been analyzed for gain more information on the crystal structure. *Figure 4* shows the superposition of IR and Raman spectra at room temperature in the 400–4000 cm^{-1} region. The assignments of the observed bands were essentially based on comparisons with data previously reported for similar compounds [27, 28].

Detailed assignments of the bands are listed in Table 4. The aromatic C-H stretching vibrations are observed in the IR spectrum at 3024 cm^{-1} and in the region 3023-3068 cm^{-1} in Raman, while that of the aliphatic CH bond were observed at 2954 and 2847 cm^{-1} in the IR spectrum and 2962; 2855 cm^{-1} in the Raman spectrum. The strong band observed at 2736 cm^{-1} in the IR spectrum may correspond to the symmetric stretching vibrations of (NH^+), whereas this band is not observed in the Raman spectra. The band appears around 1605 cm^{-1} in IR and 1603 in Raman corresponds to ν (C=C) of the aromatic ring. The bands identified at 1454 and 1409 cm^{-1} in the IR spectrum and at 1466 and 1408 cm^{-1} in the Raman spectrum are assigned to CH_3 and CH_2 deformation modes. The two peaks at 1326 and 1309 cm^{-1} are characteristic of the stretching vibration ν (CN). The deformation modes δ (C-H) of the aromatic ring occur in two bands in the IR spectrum at 1242 and 1232 cm^{-1} and at 1321 and 1265 cm^{-1} in the Raman spectrum. The bands observed in IR at 1055 and 1009 cm^{-1} are due to δ (C-C), δ (C-H) and are detected by Raman in the 1032-1003 cm^{-1} region. The frequency region between 934 and 829 cm^{-1} corresponds to δ(CH) and ρ(CH_3) and is detected in the Raman frequency between 931 and 813 cm^{-1}. The detected peak around 740 cm^{-1} in the IR spectrum

was also recorded with low intensity in the Raman spectrum is due to the vibration mode γ(CC) of the aromatic ring. Finally, the deformation vibration δ (CCC) and δ (CNC) are manifested in a series of bands in the 650-434 cm^{-1} region.

Figure 5 illustrates the Raman spectrum recorded at low frequencies (80-400 cm^{-1}) of the compound $(C_9H_{14}N)_2CoCl_4$. In this frequency range, we can observe the characteristic bands of the vibrations of the $(CoCl_4)^{2-}$ anion. Based on the spectra of compounds containing an anionic group $(CoCl_4)^{2-}$ [22, 30], we were able to make a detailed assignment of all observed vibration. Indeed, the two bands detected at 321 and 266 cm^{-1} are due to the symmetric and asymmetric stretching vibrations of the Co-Cl bonds. The bands corresponding to the deformation mode of (Cl-Co-Cl) appeared in the 163–106 cm^{-1} region. The lattice modes were observed in the Raman spectra at 84 cm^{-1}.

3.4. Magnetic Studies

The temperature dependence (T) of the magnetization (M) (*Fig. 6*) reveals that the magnetic moment increases with decreasing temperature. We can note that there is no maximunin magnetization versus temperature curves, so the antiferromagnetic–paramagnetic transition occurs at a temperature Neel (T_N) lower than 2K.

The magnetic properties are also shown in *Fig. 7*, in the form of susceptibility (χ) versus (T) plots. The low temperature magnetic susceptibility data was fit to the Curie–Weiss law, given by $\chi = \frac{C}{(T-\theta_{cw})}$. The experimental effective paramagnetic moments μ_{eff}^{exp} were calculated from $C = \left(\frac{N_A}{3K_B}\right)\mu_{eff}^2$, where C, θ_{cw}, N_A, K_B and μ_B have their usual meanings. The values of (C), (θ_{cw}) and (μ_{eff}^{exp}) as a function of the applied magnetic field were deduced from *Fig. 6* and were collected in *Table 5*.

On the other hand, the Curie–Weiss temperature θ_{CW} is given by **[31]**:

$$\theta_{cw} = Z\frac{S(S+1)J_{nn}}{3}$$

Where z is the nearest neighbor (z = 4), S is the spin of Co^{3+} ion and Jnn is the nearest neighbor interaction.

From the experimental θ_{CW} value, we have calculated the Jnn value (Jnn = −2.30 K). This negative value confirms the presence of an effective antiferromagnetic interaction among Co^{3+} ions.

As indicated by Raju et al. **[32]**, the classical nearest neighbor exchange J^{cl} and dipolar D_{nn} interactions are given by:

$$J^{cl} = S(S+1)J_{nn}$$

$$D_{nn} = \frac{\mu_{eff}^{2}\mu_{0}}{4\pi(a_0/8)^3}$$

Where a_0 is the unit cell length of $(C_9H_{14}N)_2CoCl_4$ compound.

The J^{cl} and Dnn values confirm the dominant dipolar interaction between Co^{3+} ions in the structure.

We have also studied the theoretical effective moment can be calculated as follows **[33]**:

$\mu_{eff}^{the} = g\mu_B\sqrt{J(J+1)}$;

In our case, according to our sample which contains one unpaired electron Co (II) ($3d^7$, S=5/2), we found that the value of the effective moment (μ_{eff}^{the}) is the order of $5.91\mu_B$. Such a difference between the experimental effective moment and the theoretical one can be explained by the existence of short range antiferromagnetic correlations in the paramagnetic state **[34, 35]**. The negative temperatures intercept together with the decrease of the effective magnetic moment and are in agreement with the existence of an antiferromagnetic exchange.

The *figure 8* shows the absence of hysteresis loop and also the saturation, proving the paramagnetic behavior same 5K.

4. Conclusion

The present study reports on the synthesis and subsequent characterization of a new chlorocobaltate (II), $(C_9H_{14}N)_2\,CoCl_4$. The structure of this compound consists of alternation organic and inorganic layers. The anionic layer is built up by tetrahedral of $[CoCl_4]^{2-}$ arranged in sandwich between the organic layers. These layers are themselves interconnected by means of the ionic N–H…Cl hydrogen bonds. The (TG/DSC) thermal analysis was performed to establish the thermal stability of the crystal. Moreover, the vibrational properties of this compound were studied by Raman scattering and infrared spectroscopy. Magnetic measurements revealed that the thermal variation of the magnetic susceptibility exhibited an antiferromagnetic interaction between the Co (II) centers which has been confirmed by the values of the exchange parameter. The isothermal magnetization curves with the absence of magnetic hysteresis loops, proved that the perfect magnetic reversibility of $(C_9H_{14}N)_2\,CoCl_4$ compound.

References

[1] I. Khelifa, A. Belmokhtar, R. Berenguer, A. Benyoucef, E.Morallon, J. of Mol. Struct. 1178 (2019) 327–332.

[2] W. Amamou, N. Elleuch , H. Feki , N. Chniba-boudjada , F. Zouari, J. of Mol. Struct. 1083 (2015) 168–174.

[3] K. Yamani, R. Berenguer, A. Benyoucef. E. Morallón, 135 (2019) 2089-2100.

[4] S. Benyakhou, A. Belmokhtar, A. Zehhaf, A.Benyoucef, 1150 (2017) 580-585.

[5] A. Mancini, P. Quadrelli, G. Amoroso, C. Milanese, M. Boiocchi, A. Sironi, M. Patrini, G. Guizzetti and L. Malavasi, J. Solid State Chem. 240 (2016) 55-60.

[6] Jui-Cheng Chang, Wen-Yueh Ho, I-Wen Sun, Yu-Kai Chou, Hsin-Hsiu Hsieh, Tzi-Yi Wu, Polyhedron 30 (2011) 497–507.

[7] K. Kumar Bisht, A. Cherian Kathalikkattil , S. Eringathodi, J. of Mol. Struct. 1013 (2012) 102–110.

[8] M.G. Brik, A. El-Korashy, M. Almokhtar, Journal of Alloys and Compounds 459 (2008) 71–77.

[9] M.A. Baldo, D.F. O'Brien, Y. You, A. Shoustikov, S. Sibley, M.E. Thompson, S.R. Forrest, Nature 395 (1998) 151–154.

[10] C.W. Tang, S.A. Van Slyke, Appl. Phys. Lett. 51 (1987) 913–915.

[11] B. Machura, M. Wolff, I. Gryca, R. Kruszynski, Polyhedron 40 (2012) 93–104.

[12] M. Abdalrahman, C. P. Landee, S. G. Telfer, M. M. Turnbull, J. L. Wikaira, Inorg.Chim. Acta 389 (2012) 66–76.

[13] K. Edwards , S.N. Herringer, A. R. Parent, M. Provost, K. C. Shortsleeves , M.M. Turnbull, L. N. Dawe, Inorg. Chim. Acta 368 (2011) 141–151.

[14] F. Issaoui, I. Baccar, E. Dhahri, O. El Sadek, F. Zouari, E.K. Hlil, J Supercond Nov Magn (2012), DOI 10.1007/s10948-012-1469-5.

[15] F. Issaoui, Y. Baklouti, E. Dhahri, F. Zouari, M. A. Valente, J Supercond Nov Magn. (2015) 1421-1427.

[16] R. Madar, P. Chaudouet, E. Dhahri, J.P Senateur, R. Fruchart, B. Lambert, J. Solid State Chem. 56 (1985) 335-342.

[17] P. C. Crawford, A. L. Gillon, J. Green, A. G. Orpen, T. J. Podesta and S. V. Pritchard, Cryst Eng Comm, 6 (2004) 419.

[18] C. J. Adams, A. L. Gillon, M. Lusi and A. G. Orpen, CrystEngComm, 2010, 12, 4403.

[19] L. Brammer, E.A. Bruton, P. Sherwood, Cryst. Growth Des. 1 (2001) 277.

[20] I. Baccar, F. Issaoui, F. Zouari, M. Hussein, E. Dhahri, M.A. Valente, Solid State Communications 150, (2010) 2005-2010.

[21] C. Decaroli, A. M. Arevalo- Lopez, C. H. Woodall, E. E. Rodriguez,c J. P. Attfield, S. F. Parkerd and C. Stock, Acta Cryst. B71 (2015).

[22] G.M. Sheldrick, SADABS Bruker AXS Inc., Madison, Wisconsin, USA, 2002.

[23] G.M. Sheldrick, SHELX97-2, Programs for the Solution and Refinement of Crystal Structures, University of Go¨ttingen, Germany, 1997.

[24] J.C. Chang, W.Y. Ho, I.W. Sun, Y.K. Chou, H.H. Hsieh, T.Y. Wu, Inorg. Chim. Acta 368 (2011) 141–151.

[25] W. Baur, J. Acta Crystallogr., Sect. B 30 (1974) 1191.

[26] S. Nasri, F. Zouari, H. El Feki, J. Chem. Crystallogr. 38 (2008) 729–732.

[27] M.O. Sinnokrot, E.F. Valeev, C.D. Sherrill, J. Am. Chem. Soc. 124 (2002) 10887–10893.

[28] H. Feki, Z. Elaoud, T. Mhiri, Y. Abid, A. Mlayah, Spectrochim. Acta Part A 69 (2008) 743–747.

[29] R. P. Rathore, S. S. Khatri and T. Chakraborty, J. OF Raman Spec. 18 (1987) 429-434.

[30] N. N. Greenwood, “Spectroscopic Properties of Inorganic and Organometallic Compounds” volume 6 (1973) 211.

[31]. Dasgupta, P., Jana, Y.M., Nag Chattopadhyay, A., Higashinaka, R., Maeno, Y., Ghosh, D.: J. Phys. Chem. Solids 68, (2007) 352.

[32]. Raju, N.P., Dion, M., Gingras, M.J.P., Mason, T.E., Greedon, J.E.: Phys. Rev. B 59, (1999) 14489.

[33] C.Kittel, IntroductiontoSolidStatePhysis, 6thed, Wiley, NewYork, (1985) 404–406.

[34] H.Terashita, J.J.Neumeier, Phys.Rev.B71 (2005)134.

[35] S.Zemni, A.Gasmi, M.Boudard, M.Oumezzine, Mater.Sci.Eng.B144 (2007) 117.

Table 1: Crystal data, data collection and refinement parameters.

Crystal data	
Chemical formula	$C_{18}H_{28}Cl_4CoN_2$
Formula weight (g/mol)	473.18
T (K)	293(2)
Crystal size (mm)	0.30×0.22×0.10
Crystal system,	Triclinc
Space group	P-1
a (Å)	10.459(8)
b (Å)	14.099(11)
c (Å)	16.150(12)
α (°)	88.599(2)
β(°)	88.080(2)
γ(°)	89.754(2)
v (Å^3)	2379.8(3)
Z	2
D_{calc} (g.cm^{-3})	1.354
Absorption coefficient (mm^{-1})	1.165
F(000)	1020
Diffractometer	Bruker Apex II Kappa CCD
Monochromator	Graphite
Radiation type, λ (Å)	Mo-*K*α, 0.7107 Å
Θ Range (°)	1.26 – 26.31
Indexes range	-11≤ h ≤ 11 -15 ≤ k ≤ 15 -17 ≤ l ≤ 17
Measured reflections	16462
Independent reflections	6709
Observed refl. ($I > 2\sigma(I)$)	5153
*R*int	0.051
Data/ rastraints/ parameters	5153/0/ 452
$R(F0^2) > 2\sigma(F0^2)$]	R_1=0.058 wR_2= 0.115
GooF = *S*	1.063
Δ*ρ*max/Δ*ρ*min (e Å^{-3})	0.822/ -0.799

Table 2:

Selected bond lengths (Å) and angles (deg) for $(C_9H_{14}N)_2CoCl_4$

Distance (Å)		Angles (°)	
Anion 1			
Co1-Cl1	2.276(3)	Cl1-Co1-Cl2	106.64(11)
Co1-Cl2	2.285(3)	Cl1-Co1-Cl3	106.89(12)
Co1-Cl3	2.297(3)	Cl2-Co1-Cl3	109.82(12)
Co1-Cl4	2.226(3)	Cl1-Co1-Cl4	111.10(14)
		Cl2-Co1-Cl4	112.75(14)
		Cl3-Co1-Cl4	109.44(14)
Anion 2			
Co2-Cl5	2.238(4)	Cl5-Co2-Cl6	110.82(14)
Co2-Cl6	2.262(3)	Cl5-Co2-Cl7	107.19(19)
Co2-Cl7	2.277(4)	Cl6-Co2-Cl7	108.73(13)
Co2-Cl8	2.260(4)	Cl5-Co2-Cl8	114.90(2)
		Cl6-Co2-Cl8	106.98(15)
		Cl7-Co2-Cl8	108.10(14)

Table 3: Bond length (Å) and angles (°) in the hydrogen-bonding scheme for $(C_9H_{14}N)_2CoCl_4$

D-H…A	d(D-H)	d(H..A)	<DHA	d(D..A)
N1-H1**A**...Cl3	0.910	2.260	163.25	3.142
N2-H2**A**...Cl1 [#1]	0.910	2.531	162.57	3.410
N3-H3A...Cl2 [#2]	0.910	2.394	167.55	3.288
N4-H4A...Cl5	0.910	2.528	142.53	3.297
N4-H4A...Cl7	0.910	2.989	122.81	3.565

Symmetry code: (#1) -x+1, -y, -z+1; (#2) x-1, y, z+1

Table 4: Infrared and Raman spectral data (cm^{-1}) and band assignments for $(C_9H_{14}N)_2CoCl_4$

Observed frequency (cm^{-1})		**Assignement**
FT-IR	**FT-Raman**	
-	3068	ν_{as}(CH) aromatic
3024	3023	ν_s(CH) aromatic
2954	2962	$\nu_{as}(CH_3)$
2847	2855	$\nu_{as}(CH_2)$
2744	-	$\nu_s(NH^+)$
1598	1603	ν_{as}(C=C)
1452	1460	$\delta_s(CH_3)$, δ_s (CH_2)
1407	1413	δ(CH)
-	1363	ν_{as}(C-N)
1272	-	ν (ring) + ν(C-N)
1213	1220	In-plane CH deformation mode
1167	-	ω (CH_2)
1131	-	ν_{ring}
1055	1032	δ (C−C) + δ (C−H)
1009	1003	δ_{as}(C=C)
934	934	ρ(CH3)
829	837	out-of-plane CH deformation mode
740	746	δ_s(CC)
694	-	
-	627	δ_{ring}
596	595	δ(CNC)
491	506	δ (CCC)
-	446	
-	321	ν_{as}(Co-Cl)
-	266	ν_s(Co-Cl)
-	163	δ (CoCl)
-	106	δ (Cl-Co-Cl)
-	84	Lattice modes

Table 5: Values of the Curie constant, C, the Weiss temperature θ_{cw}, and the experimental magnetic moment μ_{eff}^{exp} $(C_9H_{14}N)_2\,CoCl_4$

μ_0H(T)	0.1	0.3	0.5	1	2
C (emu K/g)	3.34	2.93	2.85	2.84	2.76
θ_{cw}(K)	-3.24	-3.15	-2.87	-2.65	-2.48
μ_{eff} (μ_B)	5.13	4.87	4.86	4.83	4.76

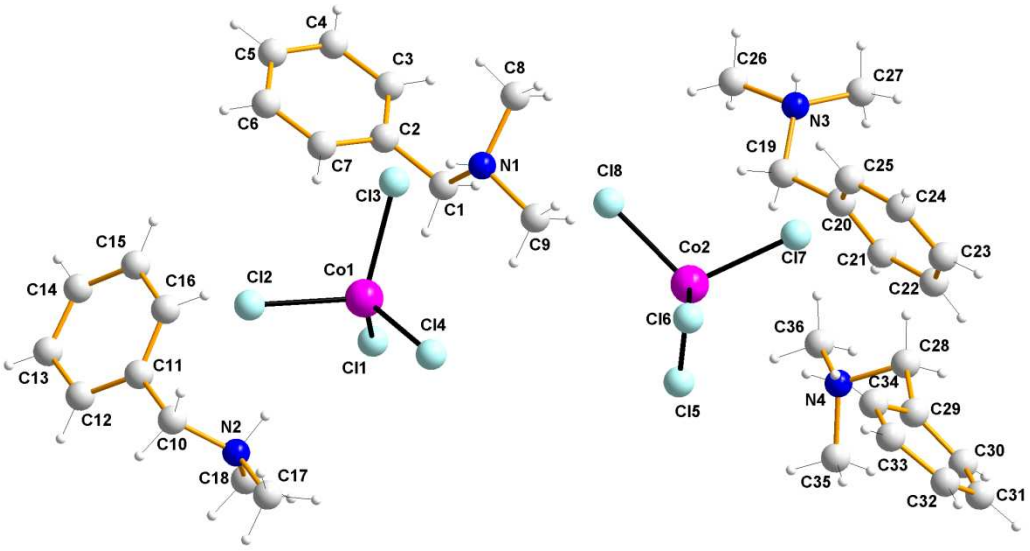

Fig. 1: The asymmetric unit of $(C_9H_{14}N)_2CoCl_4$, showing the atom-numbering scheme

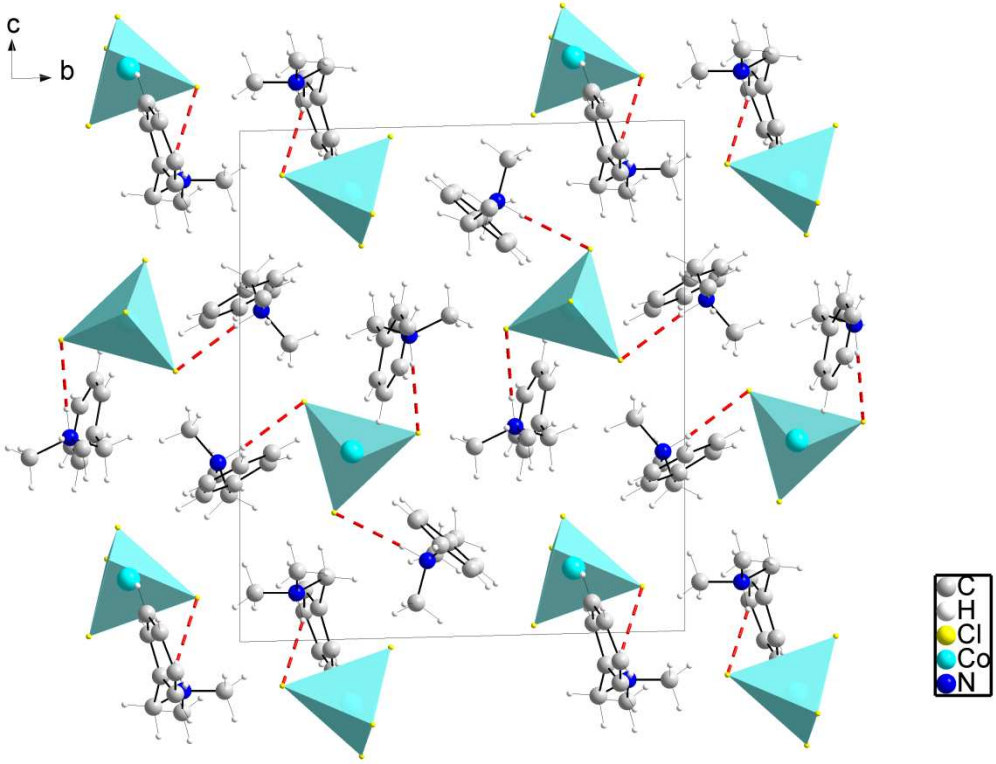

Fig.2: Projection of the crystal structure of $(C_9H_{14}N)_2CoCl_4$ in the (b, c) plane, with hydrogen bonds indicated as dashed lines.

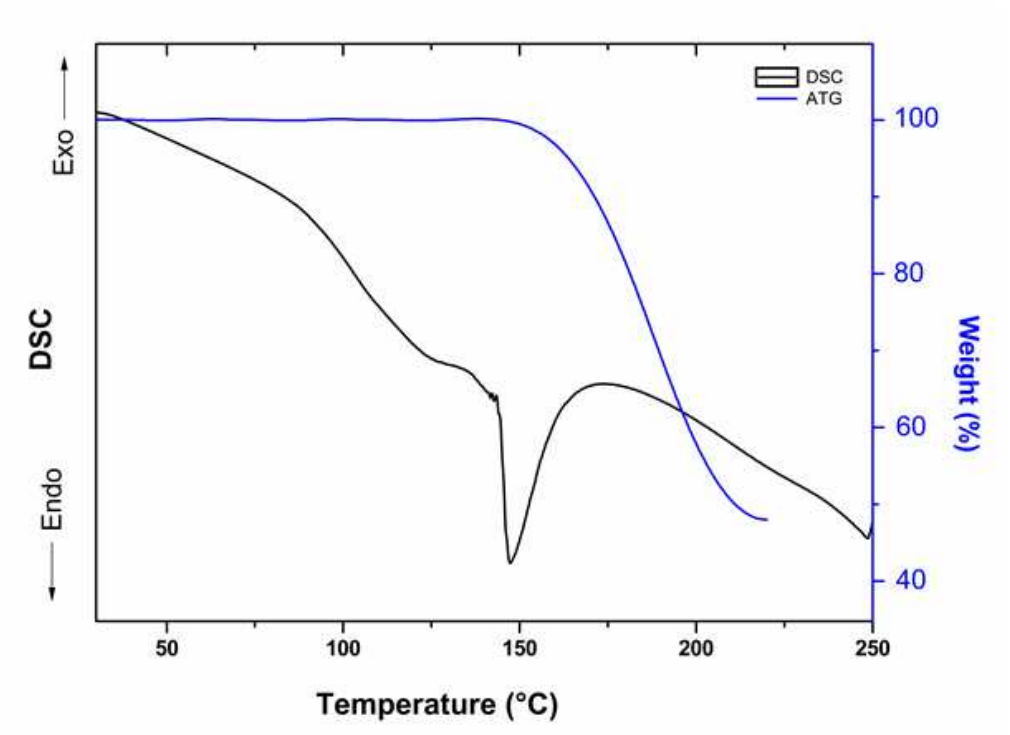

Fig.3. TG and DSC curves of $(C_9H_{14}N)_2CoCl_4$

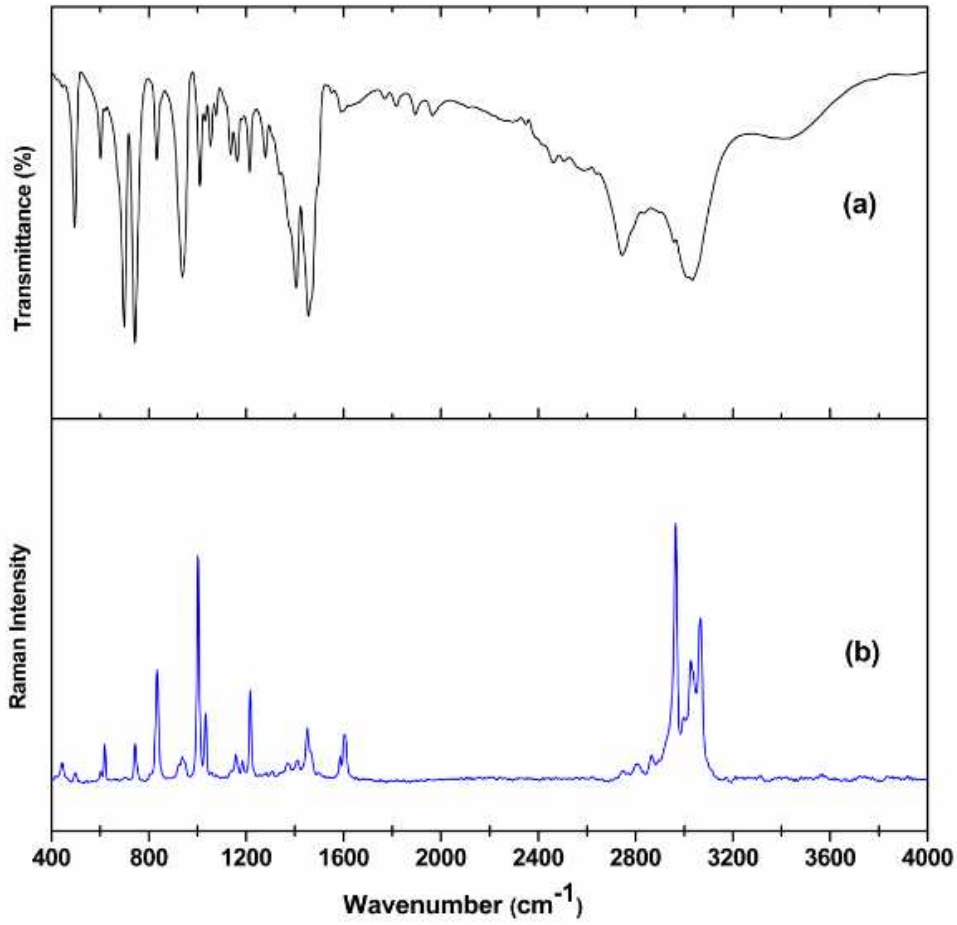

Fig.4. Superposition of (a) the IR spectra and (b) the Raman spectra at room temperature of $(C_9H_{14}N)_2CoCl_4$

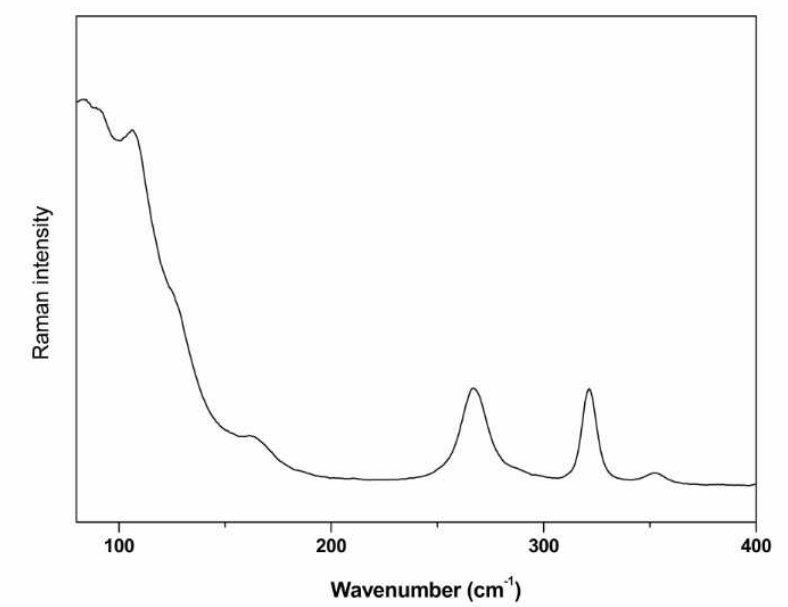

Fig.5. Raman spectrum of $(C_9H_{14}N)_2CoCl_4$ at room temperature in the 50–400 cm^{-1} region

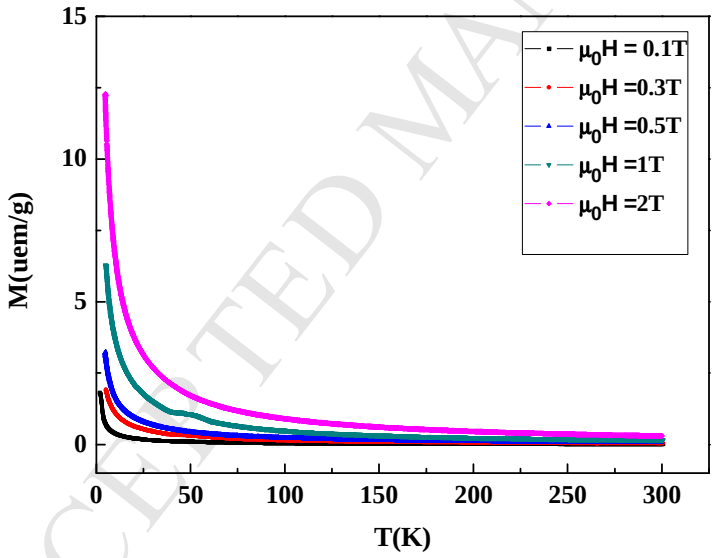

Fig.6. Variation of the magnetization as a function of temperature for different magnetic field

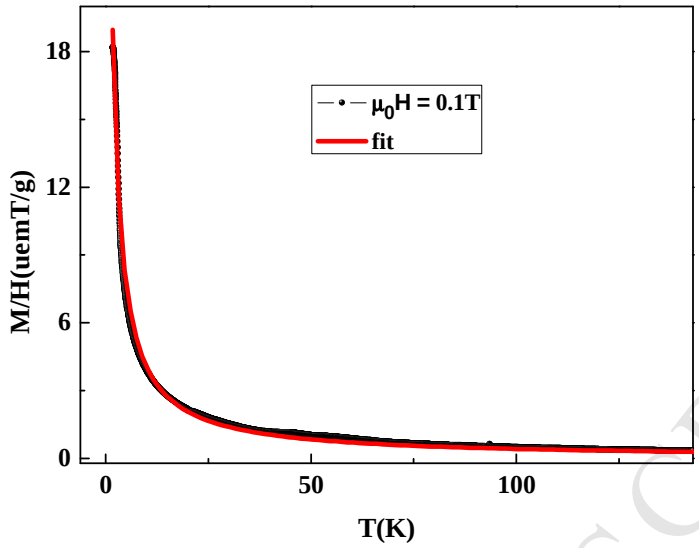

Fig.7. Thermal variation of the magnetic susceptibility of $(C_9H_{14}N)_2\,CoCl_4$ for 0.1T.

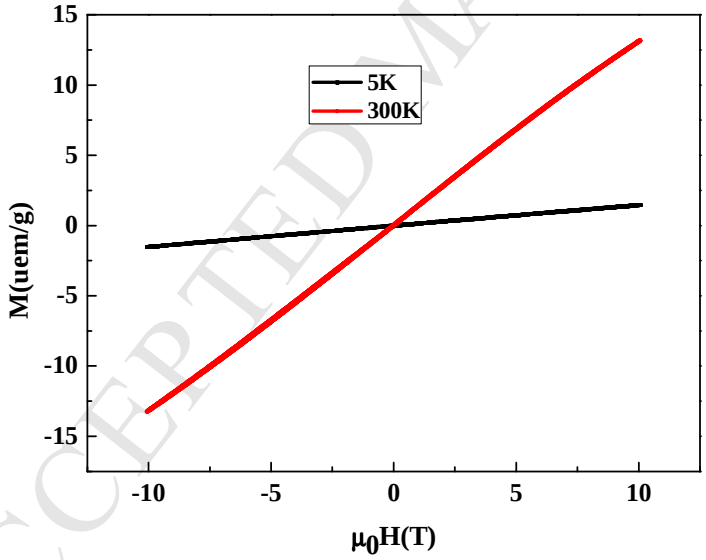

Fig.8. Hysteresis loops obtained at 5K and 300K temperature.

- The structure can be described by the alternation of organic-inorganic layers parallel to (110) plan.

- The crystal structure was stabilized by an extensive network of N-H…Cl hydrogen bonds between the cation and the anionic group $[CoCl_4]^{2-}$.

- The values of θ_{CW}, the nearest neighbor interaction Jnn , the classical nearest neighbor J^{cl} and the dipolar D_{nn} interactions' emphasize the existence of an antiferromagnetic interaction between the neighboring cobalt ions.